PROCEEDINGS, Twenty-First Workshop on Geothermal Reservoir Engineering
Stanford University, Stanford, California, January 22–24, 1996
SGP–TR–151

GEOTHERMAL FIELD'S INTERACTION WITH GEOPHYSICAL FIELDS OF ANOTHER NATURE

Oleg B. Novik*, Irina B. Mikhailovskaya+, Dmitry G. Repin♣ and Sergey V. Yershov♦

*Moscow State Geological Prospecting Academy, P.O.B. 51, Moscow 117246, Russia
+Department of Mathematics, Moscow State University, Moscow 119899, Russia
♣Department of Geological Sciences, Indiana University, 1005 East 10th Str. Bloomington IN 47405, USA
♦Keldysh Institute for Applied Mathematics, Moscow 125047, Russia

ABSTRACT

The energy balance of active lithosphere zones is to a large extent determined by nonstationary interaction of mechanical (elastic and hydrodynamic), thermal, electromagnetic, and gravitational geophysical fields. Seismic disturbances of electromagnetic and temperature fields, repeatedly observed before earthquakes are a striking manifestation of this interaction (Sec. 1).

Technological processes of exploitation of hydrothermal deposits are determined by the interaction of hydrodynamical and temperature field (Sec. 2). These "fast" interactions (with the characteristic time scale from seconds to years) take place against the background of "slow" thermomechanical interactions (time scale of Myears), the latter determining the formation of regional geothermal fields (Sec. 3).

1. MAGNETO-THERMOELASTIC INTERACTION OF GEOPHYSICAL FIELDS.

1.1. The mechanism of seismogenic disturbances of electromagnetic and temperature fields.

A whole number of domains with increased heat flow are seismically active and prove to have high electroconductivity, or rather contain large domains (characteristic length of 10÷100 km) of high electroconductivity (0.1÷0.5 S/m), as justified by numerous magnetotelluric investigations (Chamalaun and Barton, 1993; Gough, 1974). The fitness of the domains of high thermal flow, those of high seismicity and of high electroconductivity is a consequence of intensive geodynamical regime that causes fracturing of the rocks of tectonically active lithosphere zones and, therefore, the existence of a sufficient number of channels of intensive heat and mass transfer from the asthenosphere and lower floors of lithosphere to its upper ones.

Seismic monitoring of geothermal areas, being technologically necessary, requires forecasting interpretation of signals arriving at the surface which are the seismogenic disturbances of electromagnetic and temperature fields (SDETF). This interpretation can not be effective without the understanding of the physical mechanism of SDETF origination.

In this paper the SDETF are assumed to arise due to the seismically caused nonstationary deformations of low-resistivity domains, formed by transfer of ultrabasic magmas with relatively high concentration of metals into the upper floors of lithosphere.

This mechanism is further specified in Section 1.2 when setting the mathematical model. In Section 1.3 which studies numerically the disturbances of electromagnetic and temperature fields in the model low-resistivity block in the particular case of seismogenic deformation by a seismic wave falling at the block's basement, the electromagnetic and temperature image of this type of seismical activity is demonstrated.

1.2. Mathematical model of magneto-thermoelastic interaction of geophysical fields.

In this paper for the analysis of nonstationary interaction of elastic, thermal and electromagnetic fields in the presence of gravity we use the system

$$\begin{aligned} \mathcal{H}u + \mathcal{A}(u,w) &= \rho g \\ \mathcal{P}w + \mathcal{B}(u,w) &= 0 \end{aligned} \qquad (1)$$

where

1) the hyperbolic system

$$\mathcal{H}u = \rho g \qquad (2)$$

describes nonstationary deformations as a purely conservative process, ρ being the rock's density, g the gravity acceleration, $u = u(t,x)$ the displacements;

2) $w = \{H(t,x), \theta(t,x)\}$ comprises the non-mechanical (magnetic and temperature) fields, the parabolic system

$$\mathcal{P}w = 0 \qquad (3)$$

describing the magnetic and temperature diffusion in electro- and thermoconductive medium without taking into account the influence of deformations on the transfer processes;

3) the operators $\mathcal{A}(u,w)$, $\mathcal{B}(u,w)$ describe the interaction of intensive conservative (u) and dissipative (w) processes in geological medium, vanishing for weak fields, as well as for the media close to ideally elastic. Thus holding in the upper floors of the passive lithosphere zones under moderate deformations and heat flows is the "classical" description (2)–(3).

The systems of (1) type, special cases of which are hyperbolic and parabolic systems, have no type in the present mathematical classification. Let us call them conservative-dissipative systems (Novik, 1969).

Well-posedness of initial boundary value problems and their discretization for conservative-dissipative systems, including the case of the operators $\mathcal{H}$, $\mathcal{A}$, $\mathcal{P}$, $\mathcal{B}$ corresponding to nonuniform anisotropic media with memory, both when displacement current is taken into account and when it is neglected, was proved in (Novik, 1969; Mikhailovskaya and Novik, 1979; Novik, 1994). Here we confine ourselves to the operators $\mathcal{H}$, $\mathcal{A}$, $\mathcal{P}$, $\mathcal{B}$ that correspond to nonuniform isotropic electrically uncharged media of differential type in absence of displacement current (negligible for conductivities of ~ 0.1 S/m and frequencies of ~ 1 Hz) and marked processes of electric or magnetic polarization. Using then the theory of thermoelasticity for the thermomechanical interactions and electrodynamics of slowly moving media for the interaction of electromagnetic field with mechanical and temperature ones in accordance with the principles of modern physical theory of magneto-thermoelacticity (Maugin, 1988), we arrive at the following special case of the conservative-dissipative system (1) (in the SI units):

$$\mathcal{H}\boldsymbol{u} \equiv \rho \boldsymbol{u}_{tt} - \mathrm{Div}\,\hat{\sigma},$$

$$\mathcal{A}(\boldsymbol{u},\boldsymbol{w}) \equiv \nabla\left(\beta(\theta-\theta_0)\right) - \boldsymbol{j}\times\boldsymbol{B},$$

$$\mathcal{P}\boldsymbol{w} \equiv \begin{pmatrix} \boldsymbol{B}_t + \nabla\times\left(\sigma^{-1}(\boldsymbol{j}+\pi_0\nabla\theta)\right) \\ c_v\rho\theta_t - \nabla(\kappa_1\nabla\theta) - \sigma^{-1}\boldsymbol{j}(\boldsymbol{j}+\pi_0\nabla\theta) \end{pmatrix}, \qquad (4)$$

$$\mathcal{B}(\boldsymbol{u},\boldsymbol{w}) \equiv \begin{pmatrix} -\nabla\times(\boldsymbol{u}_t\times\boldsymbol{B}) \\ \beta\theta_0\nabla\boldsymbol{u}_t \end{pmatrix}$$

where $i,k = 1,\ 2,\ 3;\ \sigma_{ik} \equiv \mu\cdot\left(\frac{\partial u_i}{\partial x_k} - \frac{\partial u_k}{\partial x_i}\right) + \lambda\delta_{ik}\nabla\boldsymbol{u}$, $\left(\mathrm{Div}\,\hat{\sigma}\right)_i \equiv \sum_{k=1}^{3}\frac{\partial\sigma_{ik}}{\partial x_k}$, $\hat{\sigma}$ is the stress tensor, δ_{ik} is 1 for $i = k$ and 0 otherwise, μ_e is the magnetic permeability, μ and λ are the Lame elastic constants, $\boldsymbol{B} = \mu_e\boldsymbol{H}$ is the magnetic field induction, $\boldsymbol{j} = \nabla\times\boldsymbol{H}$ the electric current density, $\beta = (2\mu + 3\lambda)\alpha$, α being the coefficient of thermal linear expansion, c_v is the heat capacity, σ the electroconductivity, π_0 the coefficient of thermoelectric current and κ_1 the heat conductivity. These characteristics of the medium may depend on the spatial coordinate $\boldsymbol{x}$.

In the conservative-dissipative system (1), (4) the magnetic and temperature fields $\boldsymbol{H}$ and θ depend on $\boldsymbol{u}_t$, i.e. the displacement's velocity. In other words, the operator $\mathcal{B}(\boldsymbol{u},\boldsymbol{w})$ is a depending on $\boldsymbol{u}_t$ nonlinear source which "turns on" (i.e. adds to the eq. (3) for non-mechanical fields in unmovable medium) if the elastic field is destabilized substantially, as is the case for seismic activization. So, by virtue of the conservative-dissipative system at issue, the configuration of thermal and magnetic fields should be disturbed under seismic activization of the medium. Numerical results concerning the magneto-thermoelasticity (MTE) mechanism are reported below.

1.3. Numerical simulation of SDETF with the help of conservative-dissipative system (1), (4).

Let us consider the simplest scheme of the MTE mechanism of seismic disturbance of electromagnetic and temperature fields.

Let us assume that the seismoactive medium contains a uniform submerged 2D geoblock with rectangle cross-section of 10 km (horiz.) by 5 km (vert.) with relatively high electroconductivity $\sigma = 0.1$ S/m and usual from petrophysical viewpoint values of other parameters:

$\rho = 4500$ kg/m^3, $\mu = 3\cdot10^{10}$ Pa, $\lambda = 5\cdot10^{10}$ Pa,
$\mu_e = 1.592\cdot10^{-6}$ H/m, $\pi_0 = 0$, $c_v = 660$ J/(kg×K),
$\kappa_1 = 3.9$ W/(m×K), $\theta_0 = 400$ K.

Let us imagine that as a result of the activization of a seismic source beneath the block arrived at its lower basement at $t = 0$ has an elastic wave of vertical displacements with the frequency of 0.4 Hz and the amplitude of 2 cm in the basement's centre (and vanishing at its edges) which acts during 5 seconds.

Used as the boundary conditions for the magnetic and temperature fields were various modifications of the condition of conservation of a field or normal derivative on one part of the rectangle's boundary and their vanishing on another; so that (according to the 2D version of (1), (4) with constant coefficients) the stationary configuration for each non-mechanical fields is the uniform one, determined by the constant value on the boundary which is what was taken as the initial condition for the corresponding field of H_1, H_2 or θ. For the mechanical field used as the stationary configuration at $t = 0$ was the field of stationary displacements under the action of gravity, the boundary condition being that of zero displacements which are then fixed the same for all $t > 0$ on all boundaries but on the bottom one, where for $t > 0$ a vertical displacement is specified which is determined by the seismic wave arrival at the block's bottom.

Numerical simulations showed that for $t \le 0.1$ s the disturbances of all fields (at the sensitivity discrimination level of the corresponding geophysical detectors) are located in the domain adjoining that of the initial contact (the bottom's centre) of the seismic

wave with the block, but after several tenths of a second they occupy the body of the block (see Figs. 1, 2) and reach for its roof: the magnetic field by $t = 0.5$ s (at the level of 100 pT) while the elastic and temperature ones by $t = 1$ s (at the levels of 0.01 m/s and 0.0001 K respectively).

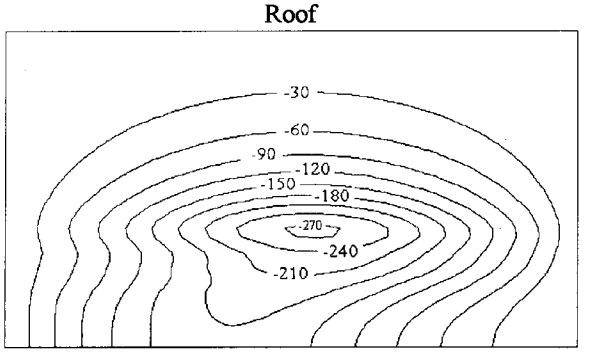

Fig. 1. Propagation (from the basement to the roof) of the seismogenic disturbances of magnetic field in the conductive model rectangle block's body. Plotted are the contours of the deviation $B_2 - B_{20}$ [pT] of the horizontal component of magnetic induction from its stationary value in 0.4 s after the seismic wave arrived at the basement.

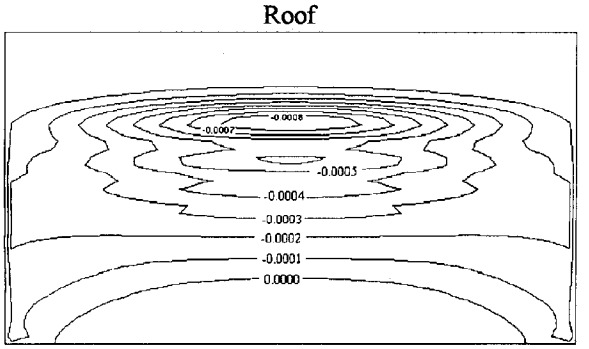

Fig. 2. The same as in Fig. 2, but for the temperature field. Plotted are the contours of the deviation $\theta - \theta_0$ [K] of the temperature from its stationary value in 0.8 s after the seismic wave arrived at the basement.

Therefore there is no doubt that the origin of the ultra-low frequency oscillations of magnetic and temperature fields (Figs. 3, 4) is due to the seismic wave arrived at the basement (and not due to, say, simulation errors). The same is confirmed by the amplification of oscillations of non-mechanical fields on the roof caused by the arrival of the second seismic wave at the basement (the amplitude of 4 cm, frequency of 0.4 Hz) at $t = 60$ s, as well as by that the peak in the spectra of electromagnetic and temperature oscillations fits the frequency of the seismic wave, falling at the basement.

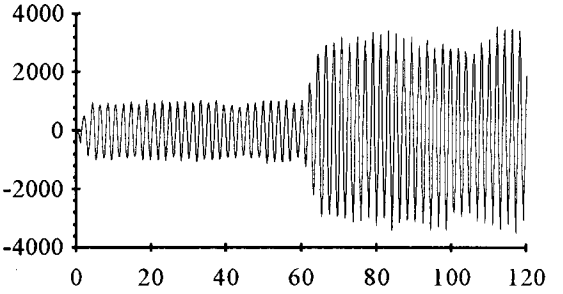

Fig. 3. The sample of electromagnetic image created by the electroconductive block out of two successive seismic waves arrived at its basement with time gap of 55 s (the first of the amplitude of 2 cm; the second of 4 cm; both have the frequency of 0.4 Hz and duration of 5 s). Plotted is the time series $B_2 - B_{20}$ [pT] at the centre of the block's roof during 120 s.

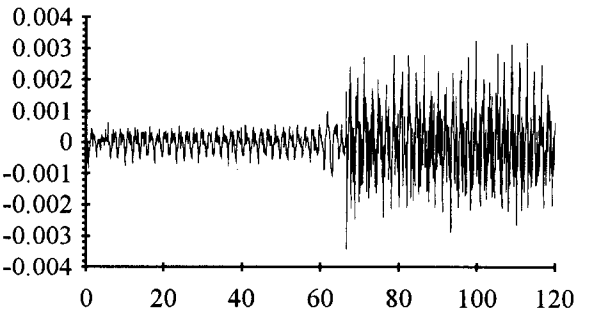

Fig. 4. The same as in Fig. 3 but for the thermal image. Plotted is the deviation $\theta - \theta_0$ [K] of the temperature from its stationary value at the centre of the block.

The calculated oscillations of the electric field and electric current are similar to that shown in Fig. 3.

The characteristics of the SDETF we calculated are in the same range as those of experimental observations (Fraser-Smith, Bernardi *et al*, 1990; Gulielmi and Levshenko, 1994). And if $\nabla\times(\boldsymbol{u}_t\times\boldsymbol{B}) \approx 0$ and/or $\nabla\boldsymbol{u}_t = 0$ the magnetic and/or temperature oscillations will not originate, which was observed as well. Also possible is the inverse case, when, say, electromagnetic oscillations are observed without seismic wave which has decayed because the decay conditions for elastic waves and electromagnetic ones of ultra-low frequency differ.

So low-resistivity domains, typical of seismically active lithosphere zones with an increased heat flow, play the role of transformers of the energy of non-

stationary deformations into low frequency electromagnetic and temperature waves, therefore being indicators of seismic activization.

Recommended for the purpose of seismological monitoring on the basis of our simulations may be observation of magnetic field in ultra low frequency band, as well as observations of temperature in bore-holes.

2. HYDRO-GEOTHERMAL FIELD INTERACTION.

2.1. The problem.

The thermal water's temperature and salt percentage depend on hydrodynamic velocity, i.e. hydro-geothermal field interaction may be of importance by intensive pumping. The mathematical setting and numerical method are considered in order to determine the optimal outputs of a system of industrial water intakes in a heterogeneous water-bearing complex. The expenditures connected in particular with lifting, transportation (turbulent resistance) and injection of the exhaust water into bore-holes must be minimized under the following restrictions: the total volumes of the heat obtained and the chemical components extracted should be within the given limits during the given period; the outputs of every intake and cone of influence (interference of intakes) should not exceed the prescribed values determined by the hydraulic pump characteristics.

2.2. The mathematical model.

The problem of rational choice of technology of thermal water deposits exploitation can be described by the following mathematical model.

Let N water intakes with outputs $\boldsymbol{Q} \equiv \{Q_1,...,Q_N\}$, which may be of different signs so an injection into the water-bearing horizon is admissible, be situated at the points (x_i, y_i), $i = 1,...,N$ of geothermal area Ω and be connected with one another and with processing plants and users by M pipelines.

The total water discharge in m-th pipeline is $\sum_{s=1}^{N} \delta_m^s Q_s$, where δ_m^s is 1 if the output of s-th intake is transported by m-th pipeline, and 0 otherwise; the matrix δ_m^s being determined by the given scheme of transportation of the water lifted to surface. Assuming square-law turbulent resistance, one obtains that the expenditures (per time unit) on operation of each pipeline are proportional to a cube of its output. Thus the total expenditures $C(\boldsymbol{Q},t_1)$ by time t_1 on lifting $(\sum_{i=1}^{N}\cdots)$, transportation $(\sum_{m=1}^{M}\cdots)$ and injection (F) of exhaust water of the density ρ which are to be minimized by the choice of $\boldsymbol{Q}$ are

$$C(\boldsymbol{Q},t_1)=\sum_{i=1}^{N}\int_0^{t_1}\alpha_i\rho g Q_i \ell_i(t,\boldsymbol{Q})dt + \sum_{m=1}^{M}\int_0^{t_1}\gamma_m\left(\sum_{s=1}^{N}\delta_m^s Q_s\right)^3 dt + F(\boldsymbol{Q},t_1) \tag{5}$$

Here $\ell_i(t,\boldsymbol{Q})$ denotes the depth from which the output of the i-th intake is lifted at time t; g is the acceleration of gravity; α_i and γ_m are technological coefficients determined by efficiency of the pumps, cost of energy, characteristics of the pipeline and its interior's condition.

Let us state the restrictions under which the outputs $\boldsymbol{Q}_*$ should be found that minimize $C(\boldsymbol{Q},t_1)$:

$$Q_i^{\min} < Q_i < Q_i^{\max}, \quad i=1,...,N; \tag{6}$$

$$\left.\begin{aligned} &\max_{t\in[0,t_1]} \ell_i(t,\boldsymbol{Q}) < \ell_i^{\max}, \\ &\ell_i(t,\boldsymbol{Q}) \equiv \bar{\ell}_i - h(t,x_i,y_i) - \sum_{j=1}^{N}\alpha_{ij}(t)Q_j \end{aligned}\right\}, \quad i=1,...,N; \tag{7}$$

$$\sum_{i=1}^{N}\int_0^{t_1} c_V\rho Q_i\theta(t,x_i,y_i,\boldsymbol{Q})dt = q_\theta \tag{8}$$

$$\sum_{i=1}^{N}\int_0^{t_1} Q_i c(t,x_i,y_i,\boldsymbol{Q})dt = q_C \tag{9}$$

The inequalities (6) express restrictions on the output of water intake which are admissible from the economical and technological viewpoints. In the inequality (7) $\bar{\ell}_i$ denotes the height of the point (x_i,y_i) where i-th water intake is situated above the horizon H_0, from which the piezometric levels are counted. By $h(t,x,y)$ we denote the level at the point (x,y) and time t, caused by natural dynamics of the initial levels $h_0(x,y)$ at time $t = 0$, that is, by changing the levels without pumping. In other words, $h(t,x,y)$ is the solution of the boundary value problem for equation of nonstationary filtration with zero source w:

$$Sh_t - \frac{\partial}{\partial x}\left(T_f\frac{\partial h}{\partial x}\right) - \frac{\partial}{\partial y}\left(T_f\frac{\partial h}{\partial y}\right) = w \tag{10}$$

$$L_h h\big|_{\partial\Omega} = \psi_h, \quad h(0,x,y) = h_0(x,y) \tag{11}$$

where $S = S(x,y)$ and $T_f = T_f(x,y)$ are hydraulic parameters of the water-bearing complex, the operator L_h and the function $\psi_h(t,x,y)$ being specified in accordance with the hydraulic regime at the boundary $\partial\Omega$, (Fried, 1975).

By $\alpha_{ij}(t)$ we denote the decrease of piezometric level at (x_i,y_i) by the time t due to the j-th water intake when operating alone. Thus $\alpha_{ij}(t)$ is the solution of (10)–(11) at the point (x_i,y_i) and time t when $w = -\delta(x - x_i, y - y_i)$, $\psi_h = 0$, $h_0 = 0$. Obviously the matrix of mutual influences of bore-holes $\alpha_{ij}(t)$ is only determined by hydraulic characteristics of the layer and its initial and boundary regime, i.e. by the values which are not varied in the given statement of the optimization problem (in a more realistic statement the layer's characteristics should optimally correspond to the information on it which is increasing while operation).

The expression $h+\sum_{j=1}^{N}\alpha_{ij}Q_j$ in (7) determines the level at the point (x_i,y_i) and time t, created by the total action of the natural filtration regime and the exploitation regime with outputs $\boldsymbol{Q}$.

The integrand in (8) where c_V is the heat capacity, and $\theta(t,x_i,y_i,\boldsymbol{Q})$ is the temperature of water at the point (x_i,y_i) and time t, specifies the amount of heat transported at the surface per unit time by i-th water intake. The left hand side of (8) should be equal to a given value of q_θ, calculated with regard to heat demand and losses. The temperature $\theta(t,x_i,y_i,\boldsymbol{Q})$ is determined by the solution $\theta(t,x,y,\boldsymbol{Q})$ of the boundary value problem for the equation of heat conduction with convective transfer under action of hydrodynamic velocity field $v(\boldsymbol{Q})\equiv v(t,x,y,\boldsymbol{Q})$ created by the natural filtration and that due to pumping:

$$c_V\rho\theta_t-\nabla(\kappa_1\nabla\theta)+\nabla(v(\boldsymbol{Q})\theta)=0 \qquad (12)$$

$$L_\theta\theta\big|_{\partial\Omega}=\psi_\theta,\quad \theta(0,x,y,\boldsymbol{Q})=\theta_0(x,y) \qquad (13)$$

Here $\kappa_1=\kappa_1(x,y)$ is the heat conductivity, the boundary operator L_θ and function $\psi_\theta(t,x,y)$ are determined by thermal regime at the boundary $\partial\Omega$, $\theta_0(x,y)$ specifies the initial temperature field of the water-bearing complex. The velocity field $v(\boldsymbol{Q})$ is calculated according to the filtration law

$$v(t,x,y,\boldsymbol{Q})=\kappa_f\nabla\left(h(t,x,y)+\sum_{j=1}^{N}Q_jh(t,x,y)\right) \qquad (14)$$

where $\kappa_f=\kappa_f(x,y)$ is the filtration coefficient, the term in the parentheses containing the already mentioned solutions of the boundary value problem (10)–(11).

In (9) $c(t,x_i,y_i,\boldsymbol{Q})$ denotes the concentration of extracted chemical component in the water of the i-th water intake at time t, where the field of concentration $c(t,x,y,\boldsymbol{Q})$ is determined by the solution of boundary value problem for the equation of convective diffusion

$$\mu_d c_t-\nabla(\kappa_d\nabla c)+\nabla(v(\boldsymbol{Q})c)=0 \qquad (15)$$

$$L_c c\big|_{\partial\Omega}=\psi_c,\quad c(0,x,y,\boldsymbol{Q})=c_0(x,y) \qquad (16)$$

Here $\mu_d=\mu_d(x,y)$ and $\kappa_d=\kappa_d(x,y)$ are the diffusion characteristics of the rocks, the boundary operator L_c and function $\psi_c(t,x,y)$ are given in accordance with the data regarding mass transfer at the contour $\partial\Omega$, $c_0(x,y)$ is the initial field of concentration of the extracted chemical component and $v(\boldsymbol{Q})$ is determined from (14).

2.3. The method.

When setting the optimization problem (5)–(16) we neglected the influence of temperature field and field of concentration on the density and viscosity of water, i.e. in the description of hydro-geothermal interaction only the action of hydrodynamical field on heat and mass transfer was taken into account, as is usually done in filtration engineering calculations. However, even in this statement the problem of optimal control over the heat and mass transfer by means of choosing outputs is rather laborious. Therefore only 2D fields were considered.

If one splits the time of projected exploitation of the deposit $[0,t_1]$ into intervals during which the temperature and concentration change only inessentially (under the outputs chosen these intervals are calculated from the equations of heat and mass transfer and can be determined by measurements) then the problem of optimal control over the heat and mass transfer reduces to a series of nonlinear problems of mathematical programming for each time interval. A periodic correction of $\boldsymbol{Q}_*$ is necessary also in connection with data about water-bearing complex making more and more accurate in the exploitation. In this connection the nonlinear restriction (7) can be replaced (with an admissible roughening) by a linear one, if we take into account the fact that the largest sinking of water $\alpha_{ij}(t)$ is reached at time t_1, and the largest natural sinking at each point (x_i,y_i) are known from calculation of $h(t,x_i,y_i)$. The resulting problem on minimisation of nonlinear function C under linear restrictions admits an effective solution by means of local (while searching for the extremum) linearization of C even when the dimension of $\boldsymbol{Q}$ is large.

The initial bringing of the vector $\boldsymbol{Q}$ into the domain of admissible values was achieved by generating its components as random numbers. Statistical procedures (finding solution of boundary value problem by means of averaging a functional of trajectories of the corresponding diffusion process) proved also useful for calculation of fields, especially for their estimation in isolated points (x_i,y_i). Optimization calculations for $N=2$, 3 coincided with exact solutions which may be easily constructed for these cases.

Using the optimization procedure described above, one can choose one of several graphs of pipeline network and locations of bore-holes.

3. CALCULATION OF REGIONAL GEOTHERMAL FIELD OF THE JAPAN SEA BASIN.

The results of the qualitative description of the interaction between heat transfer and processes of mechanical nature (i.e. sedimentation and tectonic processes) are described below, considering the Japan Sea basin as an example of a marginal sea in the most tectonically active Pacific segment. Regional geothermal fields of such structures can be considered only within the framework of the nonstationary theory of heat transfer that takes into account regional geological history.

In this work we trace schematized geologic and tectonic history of the Japan Sea basin beginning from the late Cretaceous (K_2d) (i.e. the origin time, $t_0=0$ for computational purposes is chosen to be 65 Myears ago). We consider the cross-section from the Bay of

Peter the Great throughout the Pervenets Rise, the Yamato Basin, and ending at the North Yamato Rise. The cross-section size is 425 km (length) by 35 km (depth). Two upper thin lines in Fig. 5 show the top and the bottom of the sedimentary layer, S, at $t = t_1 = 50.5$ Myears (i.e., at the end of early Miocene N_1^1, approximately 14.5 Myears ago). The next two thin lines are the beds of the "granite metamorphic", G, and the "basalt", B, layers that overlay the upper mantle, M.

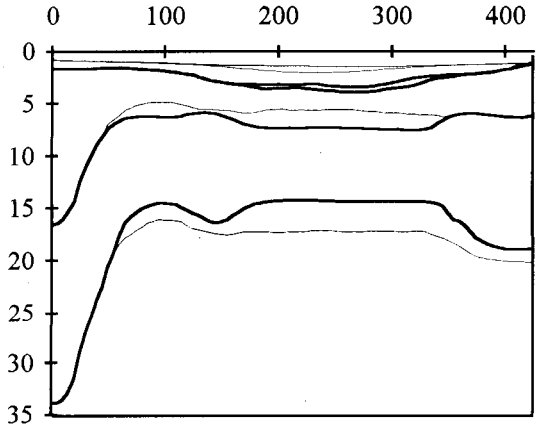

Fig. 5. Formation of the deep basinal area between early and middle Miocene. Thin lines are the upper boundaries of the layers (top to bottom) S, G, B, M at $t = 50.5$ Myears, i.e. 14.5 Myears ago (N_1^1) and thick lines show how they moved by $t = 50.7$ Myears, i.e. 14.3 Myears ago (N_1^2).

Here we assume that from the late Cretaceous (K_2d) until the end of early Miocene (N_1^1) the considered area was topographically high where sedimentary and volcanic processes had taken place accompanied by heat transfer from the mantle and internal thermal generation. Thus, the initial configuration, $D(0)$, of the developing structure $D(t)$ differs from the one shown in Fig. 5 only by the absence of the sedimentary layer, S. A short-time subsidence took place between the early Miocene, N_1^1 and the middle Miocene, N_1^2. At that time the deep basinal area was formed. The position of the boundaries of the layers at the beginning of the middle Miocene (at time $t = t_2 = 50.7$, that is, about 14.3 Myears ago) is shown in Fig. 5 by thick lines. The positions of the boundaries after a short-time post sedimentary subsidence in the late Quaternary ($64.3 < t < 65.0$) are shown by thick lines in Fig. 6. Their positions before the subsidence (i.e. at time $t_3 = 64.3$ or 0.7 million years ago) are shown in Fig. 6 by thin lines.

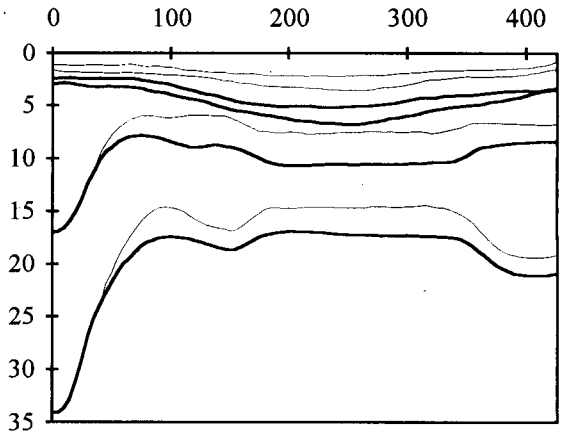

Fig. 6 The post sedimentary subsidence in the late Quaternary. Thin lines are for $t = 64.3$ Myears, i.e. 0.7 Myears ago and thick lines for $t = 65$ Myears, i.e. at the present time.

Response of heat flow through the bottom, q_b, of the basin on the previously described sequence of transformations of the basin structure was calculated by solving an initial-boundary problem for the heat transfer equation in the area $D(t)$ with moving boundaries, the top of the sedimentary layer (S), and the boundaries of basement layers (G, B, M). The horizontal heat flow was assumed to vanish on the vertical boundaries $y = 0$ and $y = l_y = 425$ km, where y is the horizontal coordinate along the profile. We set at the depth of 34 km the vertical component of the mantle heat flow as the function of y linearly decreasing from 25 mW/m^2 to 22.5 mW/m^2 on the interval of $0 < y < 170$ km and linearly increasing from this value to 35 mW/m^2 on the interval of $170 < y < 425$ km. We fixed the temperature on the top of the moving sedimentary layer to be zero. Both the stationary and strongly nonstationary initial thermal field of $D(0)$ were tested, but the Quaternary state of the field calculated does not depend considerably on variations of K_2d state. The table shows the values of the density ρ [kg/m^3], heat conductivity κ_1 [W/(m×K)], the density of the heat generation q [μW/m^3], and the heat capacity c_v [kJ/(kg×K)], used in calculations:

Layer	ρ	κ_1	q	c_v
S	2500	1.3	1.2	1.0
G	2600	2.5	0.9	1.0
B	2900	2.1	0.4	1.0
M	3300	3.2	0.04	1.0

The model parameters that were not well known were varied in relatively wide ranges. For example, thermal properties for some runs were varied from

1.5 to 2 times within areas occupying almost one fourth of the total area of the model.

These variation as well as those of the initial temperature field, seem to affect the results obtained only inessentially, so the latter seem rather reliable and representative.

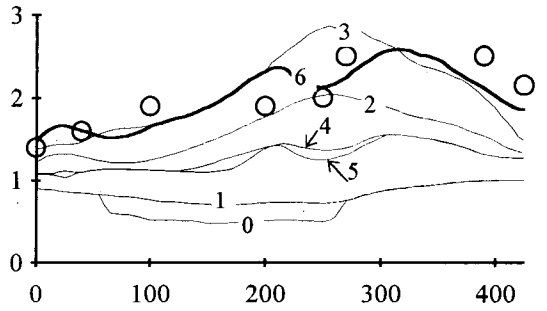

Fig. 7. Calculated evolution of the bottom heat flow's profile in the course of the geological development of the basin; the curve 6 (thick) shows the present time profile, the circles show the measured values, [HFU].

Fig. 7 shows the calculated profiles of the vertical component q_b of the heat flow through the bottom of the basin at times 0, 50.5, 50.6, 50.7, 57.0, 64.3, and 65.0 Myears, which are numbered 0, 1, 2, 3, 4, 5, 6 respectively. We see that short-time subsidence of the sea flow between N_1^1 and N_2^1 ($50.5 < t < 50.7$) lead to the increase of q_b (see curves 1, 2, 3). Then, while the boundaries of the layers were relatively stable ($50.7 < t < 64.3$), heat flow decreased (curves 4, 5). It continued to decrease until a new, relatively fast, postsedimentary subsidence took place at the late Quaternary ($t > 64.3$). This subsidence again caused a sharp increase of q_b in the present time (curve 6). Opposite to the changes in q_b, the pattern of isotherms is subjected to small changes during both subsidences. The major change in heat flow is concentrated at the depths $x < 5$ km. We conclude that the contemporary, anomalously high values of the heat flow through the bottom, which are typical for the Japan Sea, will change to the moderate ones in the future. The longer the Quaternary state of the near bottom structures and the sedimentary rate, which is connected to hydrodynamic regime, will remain stable the lower these values are going to be.

The contribution of horizontal heat flows to the formation of the regional field is insignificant because horizontal component of heat flow at the points $(x,y) \in D(t)$ for all t, $0 \le t \le 65$, does not exceed 10% of vertical component. Generalizing, we can say that the calculated values of temperature and heat flow in $D(t)$ are proportional to the mantle heat flow, q_m, because of the boundary conditions for $y = 0$, l_y, and independence of the Quaternary state of the field from the Cretaceous (K_2d) state. This suggests a small influence of heat generation on regional geothermal field formation.

The circles in Fig. 7 show the measured values of q_b (Smirnov, 1980), and curve 6 shows the calculated values, [HFU]. Taking into account the (rather low) precision of the available input information, the discussed scenario of the regional geothermal field formation leads to an acceptable correspondence to the measured field.

The tectonic transformations because of the temperature stresses depend on the thermal field evolution, the opposite influence having been demonstrated above. To describe this influence in more detail we ought to consider conservative-dissipative system of equations (Section 1.2) of the theory of thermoviscoelasticity; the numerical methods for conservative-dissipative systems with memory have been investigated in (Mikhailovskaya and Novik, 1979). But the rather complicated quantitative assumptions are necessary in this case including the initial and boundary thermo-mechanical field configurations and the space-time dependence of the rock's relaxational kernels. We believe that the above scenario considered to be acceptable due to the correspondence of the calculated heat flow and the measured one, may be used to determine these functions and to apply the viscoelastic type of motion to the problem of regional geothermal field formation together with the Navier-Stokes equations.

Considered above mathematical models of electromagnetic and thermal earthquake precursors, optimal exploitation of thermal water intakes under given volume of the heat and chemical component extracted and formation of regional geothermal fields constitute only a small part of the problem of interaction of elastic, hydrodynamic, thermal and electromagnetic fields determining the energy balance and the thermal evolution of lithosphere.

ACKNOWLEDGEMENTS

This work was partially supported by the Russian Foundation for Basic Research under grant 95–05–14775.

REFERENCES

Chamalaun, F. N. and Barton, C. E., 1993. The large-scale electrical conductivity structure of Australia. *J. Geomag. Electr.* **45**:1209–1212.

Fraser-Smith, A. C., Bernardi, A., McGill, P. R., Ladd, M. E., Helliwell, R. A., Villard, O. G., Jr., 1990. Low-frequency magnetic field measurements near the epicentre of the M 7.1 Loma Prieta earthquake. *Geophys. Res. Lett.* **17**:1465–1468.

Fried, J. J., 1975. *Ground water pollution.* Elsevier. 304 p.

Gough D. I.., 1974. Electrical conductivity under western North America in relation to heat flow, seismology and structure. *J. Geomagn. Geolectr.* **26**:105–123.

Gulielmi, A. V. and Levshenko, V. T., 1994. Electromagnetic signals from earthquakes. *Fizika Zemli* **5**:65–70 [in Russian].

Maugin, G. A., 1988. *Continuum mechanics of electromagnetic solids.* North-Holland. 560 p.

Mikhailovskaya, I. B. and Novik, O. B., 1979. The problem of Cauchy in the class of increasing functions for the non-hyperbolical system of equations which is not parabolic one. Parts I, II. *Siberian Math. Journ.* v. **21**, No. 4 (abstr.). No 2104–79 Dep., No 2105–79 Dep. All-Union Inst. Sci. & Engin. Inf.

Novik, O. B., 1969. Cauchy problem for a system of partial differential equations including a parabolic and hyperbolic operators. *Zh. Vych. Mat. i Mat. Fiz.* **9**:122–136 [in Russian].

Novik, O. B., 1994. Galerkin's method for the 3D nonlinear system of equations of magneto-thermo-elasticity. *Doklady Russ. Acad. Sci.* **334**:100–102 [in Russian].

Smirnov Ja. B., 1980. *Thermal field of the territory of the USSR.* Moscow. 150 p.